



Focused ion beam based sputtering yield measurements on ZnO and Mo thin films

E. Horváth^{a,b,*}, A. Németh^a, A.A. Koós^a, M.C. Bein^{a,b}, A.L. Tóth^a,
Z.E. Horváth^a, L.P. Biró^a, J. Gyulai^a

^a Research Institute for Technical Physics and Materials Science, H-1525, P.O. Box 49, Budapest, Hungary

^b Budapest University of Technology and Economics, H-1521, P.O. Box 91, Budapest, Hungary

Available online 8 June 2007

Abstract

In order to facilitate the lateral structuring of solar cell multilayer structures, the ion beam sputtering behaviour of Mo and ZnO thin films deposited onto soda-lime glass and single crystalline Si substrates was studied. Prior to ion beam processing the layers were analyzed by Energy Dispersive X-Ray Spectrometry (EDS), X-Ray Diffractometry (XRD) and Rutherford Backscattering (RBS). In order to characterize the ion beam sputtering of the investigated layers, $2 \times 2 \mu\text{m}^2$ fractions of the thin films were removed by a scanned 30 keV focused Ga^+ ion beam (FIB) in a dual beam system. SEM images taken during the milling process allowed continuous monitoring of the process without breaking the vacuum. The depth of the groove after removal of the layers was measured by Atomic Force Microscopy (AFM) and was plotted as a function of the ion dose. The sputtering depth has a dependence on the ion dose that is close to linear. The deviation from linearity is produced by heating effects at high beam currents. Sputtering yield values calculated from the experiments and simulations showed good agreement in the case of Mo but deviation was found in the case of ZnO.

© 2007 Elsevier Ltd. All rights reserved.

Keywords: FIB milling; Sputtering yield

1. Introduction

Solar cells are one of the most likely candidates for environmentally friendly power production. Different materials have been used for solar cell manufacturing, like crystalline Si

* Corresponding author at: Research Institute for Technical Physics and Materials Science, H-1525, P.O. Box 49, Budapest, Hungary. Tel.: +36 1 392 2222x1316; fax: +36 1 392 2226.

E-mail address: horvathe@mfa.kfki.hu (E. Horváth).

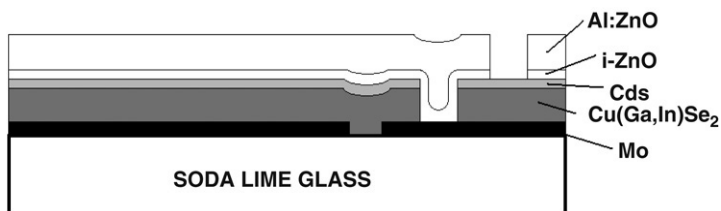


Fig. 1. Schematic cross section of the typical layer structure of a CIGS solar cell.

[1,2], poly Si [3], amorphous Si [2,4], CdTe [5], and CIGS [6], with typical energy conversion efficiencies between 6.0 and 19.2% [7,8]. For practical applications low technological costs [6, 9] are of paramount importance.

Recently, the chalcopyrite semiconductors CuInSe₂ (CIS) and Cu(In, Ga)Se₂ (CIGS) have also been used as active layers in thin film solar cells.

The layer structure of such a solar cell consists of soda-lime glass/Mo/Cu(In,Ga)Se₂/CdS/ZnO/Al:ZnO layers [10], where the soda-lime glass is used as the substrate, Mo as the back contact, CIGS as the photon absorber layer, ZnO as the buffer layer, and Al doped ZnO as the transparent front contact layer (Fig. 1).

The individual solar cells can be cut out from the multilayer CIGS panel either mechanically or by a laser process, each of them bearing some risks. Mechanical scribing can scratch the substrate glass, while laser scribing might generate rough edges. An alternative way to prepare the necessary cuts in the layer is ion-beam scribing, or using FIB processing (sputtering). With ion beams, sub-micrometre precision in positioning and roughness can be achieved, as currently used in integrated circuit manufacturing. To get more insight in the basic processes occurring during ion beam sputtering of the typical materials constituting the CIGS solar cells, a FIB study was carried out. In this paper we investigate the morphology and the beam current dependence of ion beam milling of Mo and ZnO layers, prepared by sputtering and electron beam evaporation on glass and crystalline Si substrates. In order to make use of ion beam scribing, the sputtering characteristics, such as the volume of sputtered material and possible effects arising from beam heating vs. beam current, must be accurately known. The major advantage of a cross beam FIB system is that the ion beam processing can be simultaneously monitored during the process by using a high resolution SEM without breaking the vacuum.

2. Experimental

The Mo and ZnO thin films were sputtered onto $5.5 \times 5.5 \text{ cm}^2$ glass substrates. The substrates were moved under the target with a speed of 5 cm/s in forward and backward cycles. Mo was sputtered from a metallic Mo target in Ar plasma (at a flow rate of 50 sccm) at 381 V bias and in constant power (1500 W) control mode for 20 cycles. ZnO layers were obtained by reactive sputtering from a metallic Zn target in an Ar plasma (30 sccm) with O₂ (30 sccm) at 403 V bias and in constant power (1500 W) control mode for 20 cycles. The thickness of the thin films (210 nm for Mo, and 200 nm for ZnO) was measured with a Talystep profiler.

To compare the milling characteristics of Mo layers prepared by different evaporation methods, an e-beam evaporated layer was deposited, too. The deposition rate of 1 monolayer/s in a 0.13 mPa vacuum yielded a typical thickness of 29 nm, as confirmed by Talystep measurement.

Areas of the films of $2 \times 2 \mu\text{m}^2$ were sputtered away by the scanned 30 keV focused Ga⁺ ion beam in a LEO 1540 XB cross beam system. In the experiment four different ion beam currents

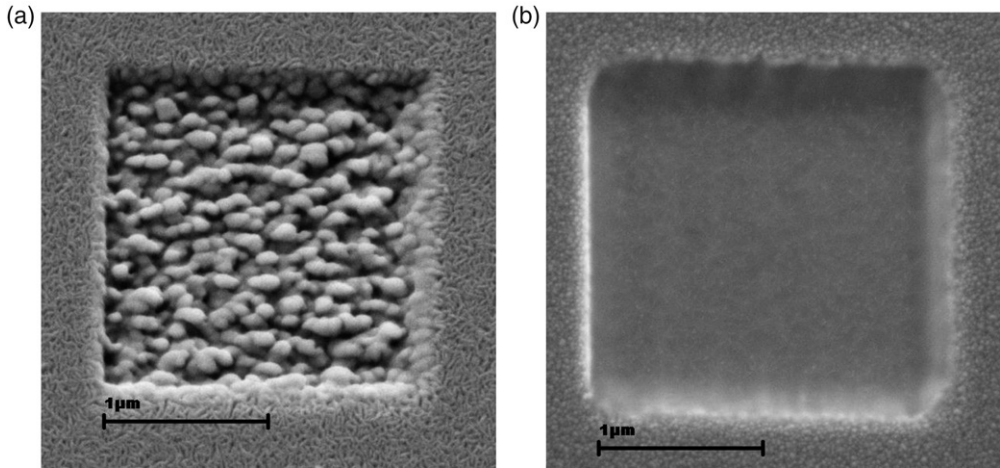


Fig. 2. SEM micrographs showing the features of the bottom of the sputtering pits produced by FIB sputtering: (a) island formation in the sputtered Mo layer; and (b) smooth surface of the sputtered ZnO layer.

(5, 10, 20, 50 pA) were selected. The milling times for each of the beam currents were chosen in such a way that the complete milling process could be investigated from the formation of a shallow pit to the complete removal of the whole film thickness. The durations were 60, 45, 30, and 15 s for Mo and 24, 18, 12, and 6 s for ZnO. For the e-beam evaporated samples, due to the thinner films, only the beam currents of 10 and 5 pA were used.

In order to select a defect free area for the experiments, the site of the milling was checked by the ion beam induced secondary electron image (FIB-SEI). During the milling, the secondary electron image of the SEM was used to monitor the process (SEM-SEI) in cross beam, i.e. tilted, position. After milling, SEM-SEI images were also used to observe the morphology of the milled pit in top view. The impurity content of the sample was determined by a built-in energy dispersive X-ray spectrometer (SEM-EDS), without breaking the vacuum using 25 kV primary electron energy.

For quantitative measurements of the milling depth, AFM measurements were performed with a VEECO NanoScope IIIa instrument operated in tapping mode using Si tips. Average values, together with minimum and maximum depths, were determined.

For the analysis of phase-composition XRD measurements were performed using a Bruker D8 Discover X-ray diffractometer with Cu K_{α} radiation ($\lambda = 0.15406$ nm) operated at 40 kV, 40 mA.

RBS measurements with 1 MeV $^4\text{He}^+$ ions, using a backscattering angle of 165° , were performed to determine the composition of the thin sputtered or evaporated films and the heavy impurities present in the layers. The recorded spectra were simulated by RBX code [11].

3. Results and discussion

The SEM study revealed the different etching behaviours of Mo and ZnO films. Both the sputtered and evaporated Mo films exhibited a rough texture at the bottom of the pit while the ZnO thin film showed a smooth surface (Fig. 2). The roughening can be attributed to the random orientation of the crystallites in the film in combination with anisotropy, i.e. different sputtering rates on different facets.

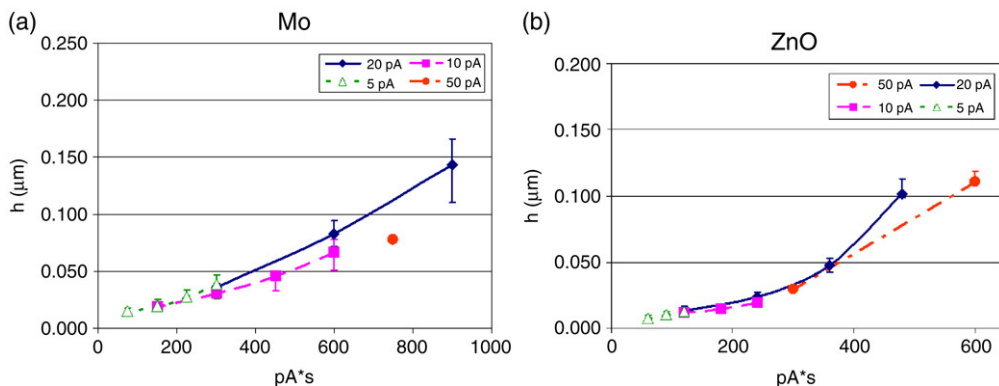


Fig. 3. Depth of the sputtered pits measured by AFM vs. ion dose: (a) for Mo and (b) for ZnO, respectively.

The AFM measurements revealed that the Mo layer milled with 50 pA was perforated, and the Mo/substrate interface was crossed. Therefore, those values were excluded from the calculation of sputtering rate. In the case of ZnO, the lowest ion current (5 pA) milled a shallow feature of <7 nm, this also was not taken into account in the sputtering calculations. The values of measured depths versus ion dose exhibit only a moderate deviation from linear behavior (see Fig. 3), which becomes more pronounced at higher doses associated with heating effects. The deviation from linearity is somewhat stronger in the case of ZnO as compared with Mo. This again may be associated with the weaker heat dissipation in the ZnO layer as compared with the Mo. The fact that the curves overlap shows that the milling depth of a certain desired geometry can be achieved with a predicted ion dose, either by slow milling with low current or by milling with a higher current for a shorter time (Fig. 3).

Depth values and the parameters of milling sputtering yield values were calculated from the AFM measurements. Typically $516\text{--}658 \mu\text{m}^3/\mu\text{A s}$ and $438\text{--}503 \mu\text{m}^3/\mu\text{A s}$ were obtained for Mo and ZnO, respectively. The averages of these values were converted into atom/ion yield values to facilitate a comparison with TRIM simulation (6.01 Mo atoms, and 3.22 ZnO molecules per impinging Ga ion).

EDS measurements were used to check the purity of the sputtered and evaporated films. They did not reveal impurity associated ones but only peaks characteristic for the materials which the sample layer (Mo, Zn) and the substrates (Si, soda-lime-glass) are composed of.

XRD measurements showed that both Mo layers are cubic (PDF Nr: 42-1120) with preferred orientation: ($hh0$) type lines are stronger than in the case of random orientation and the (200) line is missing. The ZnO layers are textured, only the (00ℓ) lines of hexagonal (PDF no. 36-1451) structure are present.

RBS measurements proved that no argon or metallic impurities are present in the films. The composition of the layers was also determined. The ZnO films are non-stoichiometric but oxygen-rich, their composition was obtained as $\text{Zn}_1\text{O}_{1.2}$. In the case of Mo films, the spectrum reflects the contribution of some light elements. From our conventional RBS experiment it is impossible to determine what kinds of light elements (lighter than nitrogen) are present in the samples, hence the assumed composition of the film is given as $\text{Mo}_1\text{C}_{0.3}$. The significant light element contamination found is tentatively attributed to carbon, the most likely impurity lighter than N originating from the vacuum system. In the sputtering yield calculations this contamination has to be taken into account.

The Transport of Ions in Matter (TRIM) [12] simulation was used to simulate the sputtering effect of 30 kV Ga ions in 210 nm Mo and 200 nm ZnO layers. In both cases 14 000 bombarding ions were considered. The simulations resulted in 5.46 Mo atoms sputtered/Ga ion at standard values, and 12.41 ZnO molecules/Ga ion (7.86 for Zn and 4.55 for O) using a density of 5.67 g cm^{-3} . While the measured and the simulated values, despite the light impurity found by RBS, agree reasonably well in the case of Mo, a discrepancy between the measured and simulated values is obtained for ZnO. This may originate from the way in which the TRIM program handles the target: it is considered that the target is not modified as a result of the ion beam processing, i.e., all incoming ions hit the same amorphous target. If the components of a compound target have different sputtering yields, as in the case of ZnO due to the different atomic masses, the changes in the composition of the target cannot be taken into account by the TRIM program.

4. Conclusion

Sputtering characteristics of Mo and ZnO thin films used in solar cell technology were investigated using a FIB system. The use of the cross beam FIB system allowed the simultaneous monitoring of the process without breaking the vacuum. It was found that ion milling may prove to be a useful tool for scribing solar cells.

The milling of Mo thin films, irrespective of their preparation technology (sputtering from metallic Mo target, e-beam evaporation of metallic Mo), led to island formation, indicating that certain crystal orientations are sputtered preferentially.

For the investigated thin films, the milling depth versus ion dose function reflects a close to linear relationship. At a given geometry the milled depth may slightly increase with increasing dose, when high beam currents are used. This anomalous increase in the sputter depth is ascribed to beam heating effects.

The experimental results are in good agreement with TRIM simulations for Mo, while a less good agreement was obtained for ZnO. The discrepancy between experimental and simulated data for ZnO is attributed to changes in the composition of the layer during sputtering.

Acknowledgements

This work was partly supported by the OTKA grant T 049131, and by the grant NKFP 3/025/2001 of the Hungarian National Office of Technology Development. The help of G. Battistig and Z. Zolnai with RBS measurements, of G. Molnár with sample preparation and of I. Bársony for useful discussions is gratefully acknowledged.

References

- [1] S. Nishida, K. Nakagawa, M. Iwane, Y. Iwasaki, N. Ukiyo, M. Mizutani, T. Shoji, *Sol. Energy Mater. Sol. Cells* 65 (2001) 525.
- [2] M. Konagai, T. Tsushima, M. Kim, K. Asakusa, A. Yamada, Y. Kudriavtsev, A. Villegas, R. Asomoza, *Thin Solid Films* 395 (2001) 152.
- [3] K. Yamamoto, M. Yoshimi, Y. Tawada, Y. Okamoto, A. Nakajima, S. Igari, *Appl. Phys. A* 69 (1999) 179.
- [4] K. Arima, T. Shigetoshi, H. Kakiuchi, M. Morita, *Physica B* 376–377 (2006) 893.
- [5] M. Burgelman, J. Verschraegen, S. Degrave, P. Nollet, *Thin Solid Films* 480–481 (2005) 392.
- [6] M. Kaelin, D. Rudmann, F. Kurdesau, H. Zogg, T. Meyer, A.N. Tiwari, *Thin Solid Films* 480–481 (2005) 486.
- [7] P.J. Rostan, U. Rau, V.X. Nguyen, T. Kirchartz, M.B. Schubert, J.H. Werner, *Sol. Energy Mater. Sol. Cells* 90 (2006) 1345.
- [8] J.H. Werner, J. Mattheis, U. Rau, *Thin Solid Films* 480–481 (2005) 399.

- [9] A. Shah, J. Meier, A. Buechel, U. Kroll, J. Steinhauser, F. Meillaud, H. Schade, D. Dominé, *Thin Solid Films* 502 (2006) 292–299.
- [10] J. Hermann, M. Benfarah, S. Bruneau, E. Axente, G. Coustillier, T. Itina, J.-F. Guillemoles, P. Alloncle, *J. Phys. D: Appl. Phys.* 39 (2006) 453–460.
- [11] E. Kótai, *Nuclear Instrum. Methods B* 85 (1994) 588.
- [12] J.F. Ziegler, J.P. Biersack, *SRIM.com*, 2003.